


Antibiotics-Induced Depletion of Rat Microbiota Induces Changes in the Expression of Host Drug-Processing Genes and Pharmacokinetic Behaviors of CYPs Probe Drugs[§]

Haijun Yang, Yanjuan Zhang, Rong Zhou, Tianyuan Wu, Peng Zhu, Yujie Liu, Jian Zhou, Yalan Xiong, Yanling Xiong, Honghao Zhou, Wei Zhang,  Yan Shu, Xiong Li, and Qing Li

Department of Clinical Pharmacology, Xiangya Hospital, Central South University, Changsha, China (H.Y., Y.Z., R.Z., T.W., P.Z., Y.L., J.Z., Yalan X., Yanling X., H.Z., W.Z., Q.L.); Institute of Clinical Pharmacology, Hunan Key Laboratory of Pharmacogenetics, Central South University, Changsha, China (H.Y., Y.Z., R.Z., T.W., P.Z., Y.L., J.Z., Yalan X., Yanling X., H.Z., W.Z., Q.L.); Engineering Research Center of Applied Technology of Pharmacogenomics, Ministry of Education, Changsha, China (H.Y., Y.Z., R.Z., T.W., P.Z., Y.L., J.Z., Yalan X., Yanling X., H.Z., W.Z., X.L., Q.L.); National Clinical Research Center for Geriatric Disorders, Changsha, China (H.Y., Y.Z., R.Z., T.W., P.Z., Y.L., J.Z., Yalan X., Yanling X., H.Z., W.Z., Q.L.); Department of Pharmaceutical Sciences, School of Pharmacy, University of Maryland at Baltimore, Maryland (Y.S.); and Key Specialty of Clinical Pharmacy, The First Affiliated Hospital of Guangdong Pharmaceutical University, Guangzhou, China (X.L.)

Received October 16, 2022; accepted December 16, 2022

ABSTRACT

The metabolism of exogenous substances is affected by the gut microbiota, and the relationship between them has become a hot topic. However, the mechanisms by which the microbiota regulates drug metabolism have not been clearly defined. This study characterizes the expression profiles of host drug-processing genes (DPGs) in antibiotics-treated rats by using an unbiased quantitative RNA-sequencing method and investigates the effects of antibiotics-induced depletion of rat microbiota on the pharmacokinetic behaviors of cytochrome P450s (CYPs) probe drugs, and bile acids metabolism by ultra-performance liquid chromatography-tandem mass spectrometry. Our results show that antibiotics treatments altered the mRNA expressions of 112 DPGs in the liver and jejunum of rats. The mRNA levels of *CYP2A1*, *CYP2C11*, *CYP2C13*, *CYP2D*, *CYP2E1*, and *CYP3A* of CYP family members were significantly downregulated in antibiotics-treated rats. Furthermore, antibiotics treatments also resulted in a significant decrease in the protein expressions and enzyme activities of

CYP3A1 and *CYP2E1* in rat liver. Pharmacokinetic results showed that, except for tolbutamide, antibiotics treatments significantly altered the pharmacokinetic behaviors of phenacetin, omeprazole, metoprolol, chlorzoxazone, and midazolam. In conclusion, the presence of stable, complex, and diverse gut microbiota plays a significant role in regulating the expression of host DPGs, which could contribute to some individual differences in pharmacokinetics.

SIGNIFICANCE STATEMENT

This study investigated how the depletion of rat microbiota by antibiotics treatments influences the expression profiles of host DPGs and the pharmacokinetic behaviors of CYPs probe drugs. Combined with previous studies in germ-free mice, this study will improve the understanding of the role of gut microbiota in drug metabolism and contribute to the understanding of individual differences in the pharmacokinetics of some drugs.

Introduction

The intestinal tract is the body's largest microecosystem, hosting a large number of intestinal microbial populations, known as "intestinal flora" (Sommer et al., 2015). It is estimated that the human gut hosts at

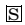
least 100 trillion microbes, including bacteria, archaea, viruses, and fungi. The number of these microorganisms is roughly equal to the number of human cells, and the number of unique genes encoded by these microorganisms is more than 100 times that of the human genome (Qin et al., 2010; Sender et al., 2016; Sepich-Poore et al., 2021). It has been reported that symbiotic intestinal microbes play an important role in promoting nutrient digestion and absorption, intestinal mucosal barrier protection, drug metabolism, and innate immune response and are closely related to the occurrence and development of a variety of diseases (Valdes et al., 2018; Savage, 2020).

In recent years, the effects of gut microbiota on the response and metabolism of exogenous substances have aroused great interest, which has led to a boom in the field of pharmacomicrobiomics (Sharma et al., 2019). Intestinal microorganisms can improve the efficacy and safety of

This study was supported by the National Natural Science Foundation (NNSF) of China [Grant 81973401]; the National Key Research and Development Program of China [Grant 2021YFA1301200]; and the National Key Clinical Specialty Construction Project (Clinical Pharmacy) and High-Level Clinical Key Specialty (Clinical Pharmacy) in Guangdong Province.

The authors report no potential conflict of interest.

dx.doi.org/10.1124/dmd.122.001173.

 This article has supplemental material available at dmd.aspetjournals.org.

ABBREVIATIONS: AUC, area under the concentration-time curve; BAs, bile acids; C_{max} , maximum concentration; CYP, cytochrome P450; DPGs, drug-processing genes; FDR-BH, Benjamini-Hochberg false discovery rate adjustment; FPKMs, fragments per kilobase of exon per million reads mapped; GF, germ-free; IS, internal standard; LCA, lithocholic acid; mRNA, messenger RNA; MRT, mean residence time; PK, pharmacokinetic; RNA-Seq, RNA-sequencing; RT-qPCR, reverse transcription-quantitative real-time polymerase chain reaction; SPF, specific pathogen-free; $t_{1/2}$, eliminate half-life; T_{max} , time to reach C_{max} ; UPLC-MS/MS, ultra-performance liquid chromatography-tandem mass spectrometry.

drugs by changing drugs structures enzymatically, thereby changing the bioavailability, bioactivity, or toxicity of drugs (Koppel et al., 2017). For example, the intestinal *Eggerthella lenta* was critical for digoxin degradation and inactivation, and its metabolic activity was related to the cardiac glycoside reductase (*cgr*) gene cluster carried by the strain (Haiser et al., 2013). In addition, the advanced colorectal cancer patients who received treatment with irinotecan exhibited a symptom of severe diarrhea, which was caused by β -glucuronidase produced by intestinal flora to catalyze the reactivation of the inactivated metabolite SN-38-G into active SN-38 (Roberts et al., 2013).

On the other hand, gut microbiota can also indirectly affect drug metabolism through their metabolites, such as bile acids (BAs), as ligands of nuclear receptors to regulate the expression of host drug metabolism enzymes and transporters [collectively known as drug-processing genes (DPGs)]. It has been shown that the expression of *Cyp3a* in the liver of germ-free (GF) mice was regulated by gut flora compared with specific pathogen-free (SPF) mice (Toda et al., 2009b). Furthermore, gene expression in GF and normal C3H/Orl mice was investigated, and it was found that the expression levels of *Cyp2c29*, *Cyp3a11*, and *Cyp8b1* messenger RNA (mRNA) were significantly reduced in GF mice. However, after 20 days of intestinal bacteria colonization and adaptation, the levels of *Cyp2c29*, *Cyp3a11*, and *Cyp8b1* in GF mice were no longer lower than those in conventionally raised mice (Claus et al., 2011). To deeply and extensively characterize the effects of intestinal microorganisms on the mRNA expressions of DPGs in GF mice, researchers comprehensively analyzed the mRNA expressions of DPGs in GF and conventional C57BL6 mice using unbiased quantitative RNA-sequencing (RNA-Seq) method (Selwyn et al., 2015). The gut microbial population and the host jointly affect the metabolism of drugs, but the specific mechanism is unclear.

Antibiotics, as the most widely used drugs in the world, have become an important force in the fields of anti-inflammatory, sterilization, and anti-infection by virtue of their powerful inhibition and lethality to bacteria (Van Boeckel et al., 2014). However, most commonly used antibiotics do not discriminate between friend and foe and have a wide spectrum of action, not only eliminating harmful bacteria but also destroying the normal flora in the human gut. Studies have shown that, after the use of most antibiotics, the amount of intestinal flora can be seriously affected for up to several months (Jernberg et al., 2010). Researchers have used broad-spectrum antibiotics to deplete the gut microbiota to construct pseudo-germ-free mice in recent years (Kennedy et al., 2018). Therefore, it is necessary to use this model to explore the influence of intestinal microbiota ecological imbalance caused by broad-spectrum antibiotics on the response and metabolism of exogenous substances, which will help us deepen understanding of the harm caused by antibiotic abuse or long-term use and understand the potential mechanism of antibiotic-drug interaction.

The purpose of this study was to evaluate whether depletion of gut microbiota by antibiotics could influence the mRNA expressions of host DPGs. Furthermore, phenacetin (rat *CYP1A2*), tolbutamide (rat *CYP2C6*), omeprazole (rat *CYP2C11*), metoprolol (rat *CYP2D1*), chlorzoxazone (rat *CYP2E1*), and midazolam (rat *CYP3A1*) were selected as core cocktail probe drugs to evaluate whether antibiotics treatments changed the pharmacokinetics of probe drugs and the corresponding cytochrome P450 (CYPs) metabolic enzyme activities in rats (Martignoni et al., 2006; Huang et al., 2014; Zhang et al., 2016). Finally, whether these effects were mediated by the regulation of host bile acid metabolism was preliminarily elucidated.

Materials and Methods

Reagents

Phenacetin, tolbutamide, and omeprazole were purchased from Sigma Aldrich (Shanghai, China); chlorzoxazone from MedChemExpress (New Jersey, USA); midazolam from Jiangsu Enhua Pharmaceutical Co., Ltd (Jiangsu, China); metoprolol and glycyrrhetic acid from Yuanye Biotechnology Co., Ltd (Shanghai, China); acetaminophen, 4-hydroxytolbutamide, 5-hydroxyomepreole, 6-hydroxy-chlorzoxazone, and 1-hydroxymidazolam from iPhase Pharmaceutical Services (Beijing, China); α -hydroxymetoprolol from Toronto Research Chemicals (Toronto, Canada). Metronidazole, neomycin trisulfate salt hydrate, vancomycin hydrochloride, ampicillin sodium salt, and amphotericin B were obtained from Sangon Biotech Co., Ltd (Shanghai, China). *CYP3A1(P6)* and *CYP2C6 (K1)* monoclonal antibodies were bought from Santa Cruz Biotechnology (California, USA); *CYP1A2*, *CYP2D1*, and *CYP2C11* polyclonal antibody from Bioss (Beijing, China); *CYP2E1* polyclonal antibody and *GAPDH* monoclonal antibody from Proteintech (Wuhan, China).

Treatment With Antibiotics

Male Wistar rats (SPF, Certificate No. 20180006033114), 200 ± 20 g, were housed in the SPF animal facilities of the Animal Experimental Center of Central South University and provided a 12-hour light/dark cycle environment, with temperature controlled at 20 to 25°C and humidity controlled at $50 \pm 10\%$. Wistar rats were treated with a mixture of antibiotics (ampicillin 20 g/L, neomycin sulfate 20 g/L, vancomycin 10 g/L, metronidazole 20 g/L, and amphotericin B 0.2 g/L) for 2 weeks to deplete the intestinal flora of recipient rats, while the wild-type rats were given the same amount of normal saline. The dosage of intra-gastric liquid was 5 mL/kg (Wu et al., 2019). To determine antibiotics-induced intestinal dysbiosis, the feces were collected weekly and the fecal microbial DNA was isolated from collected samples using the QIAamp PowerFecal Pro DNA Kit. The intestinal microbe genomic DNA was measured by Nanodrop2000 to evaluate the number of gut microbes (Guo et al., 2020). All experimental procedures were approved ethically by the Administration Committee of Experimental Animals of Central South University (Approval No. 2021SYDW0237, Changsha, China).

Biochemical Assay

Whole blood samples were collected from rats, and the serum was separated by centrifugation and stored at -80°C for further analysis. Serum alanine transaminase, aspartate aminotransferase, total bilirubin, alkaline phosphatase, albumin, gamma-glutamyl transpeptidase, total cholesterol, triglyceride, blood urea nitrogen, glucose, and creatinine were measured by Wuhan Servicebio Technology Co., Ltd. (Wuhan, China).

Histopathological Assay

The rats were sacrificed at the end of the experiment, and the large lobe of the liver, small intestine, and right kidney were quickly excised and fixed in 4% paraformaldehyde for 24 hours. After gradient dehydration, paraffin embedding and continuous sections (thickness: 4 μm) were performed. Finally, H&E staining was used to evaluate pathologic changes.

RNA-Sequencing for Host DPGs Expression Profiles

Total RNA was isolated from liver and jejunum tissues using Trizol. Total RNA was quantified by NanoDrop2000. To assess the quality of the RNA, the sample was run on an RNase-free agarose gel electrophoresis. RNA integrity number was evaluated with an Agilent 2100 Bioanalyzer. The establishment of the cDNA library and RNA sequencing were performed by Beijing Novogene Bioinformatics Technology Co., Ltd. First, raw data of fastq format was possessed through in-house perl scripts, which was to remove low-quality reads, reads containing adapter, and reads containing ploy-N to obtain clean reads (Jing et al., 2018). Paired-end clean reads were aligned onto the reference genome sequence of *rattus norvegicus* using Hisat2 v2.0.5. The mRNA abundance was quantified as fragments per kilobase of exon per million reads mapped (FPKM). Differential expression analysis between wild-type rats and antibiotics-treated rats was performed using the DESeq2 R package (1.20.0). Genes with an adjusted P value < 0.05 [namely Benjamini-Hochberg false discovery rate adjustment (FDR-BH) < 0.05] were assigned as differentially expressed. RNA-Seq

data were uploaded to the Gene Expression Omnibus database with accession number GSE199117.

Reverse Transcription-Quantitative Real-Time Polymerase Chain Reaction

Total RNA was reverse-transcribed to cDNA using a PrimeScript RT reagent Kit with gDNA Eraser (Takara). The cDNAs were used as templates for quantitative polymerase chain reaction with SYBR Green (Bimake). The reverse transcription-quantitative real-time polymerase chain reaction (qRT-PCR) assay was performed using ABI QuantStudio 5 Real-Time PCR System (Thermo Fisher). The PCR primers were synthesized by Sangon Biotech (Shanghai, China), and listed in Supplementary Table 1. The relative gene expression was analyzed using the $2^{-\Delta\Delta Ct}$ method and normalized to the expression of the housekeeping genes *GAPDH*.

Pharmacokinetic Experiments

After 2 weeks with antibiotics treatments and fasting for at least 12 hours before oral administration, the mixture of six drugs—phenacetin (10 mg/kg), tolbutamide (1 mg/kg), omeprazole (10 mg/kg), metoprolol (10 mg/kg), chlorzoxazone (1 mg/kg), and midazolam (10 mg/kg)—were given intragastrically in the manner of cocktail (Guo et al., 2022). Blood samples were collected in 200 μ L heparinized Eppendorf tubes after 0, 0.08, 0.17, 0.25, 0.33, 0.5, 0.75, 1, 2, 4, 6, 8, and 24 hours. The blood sample was centrifuged and the supernatant plasma was collected and stored at -80°C for further analysis. Relating to the preparation of blood samples, in brief, 120 μ L acetonitrile containing 20 ng/mL glycyrrhetic acid and 10 ng/mL lamotrigine [internal standard (IS)] was added to 40 μ L rat plasma samples in a 1.5 mL EP tube. The mixture was then vortexed for 5 minutes and centrifuged at 14,000 rpm for 10 minutes to precipitate and remove the proteins. Finally, 80 μ L supernatant was taken for ultra-performance liquid chromatography-tandem mass spectrometry (UPLC-MS/MS) analysis.

Ultra-Performance Liquid Chromatography-Tandem Mass Spectrometry

The concentrations of all probe drugs in plasma samples were quantified by UPLC-MS/MS. Chromatographic separations were performed with a C18 column 5 μ M packing material, 150 mm \times 2.0 mm (Phenomenex). The gradient of the chromatographic condition was as follows: 0 to 0.2 minutes, 10% B; 0.2 to 3.5 minutes, linear gradient from 10% to 90% B; 3.5 to 4.5 minutes, 90% B; 4.5 to 4.6 minutes, linear gradient back to 10% B; 4.6 to 8 minutes, 10% B. Mobile phase A is 0.1% formic acid water and mobile phase B is acetonitrile. The flow rate is 0.35 mL/min, and the injection volume was 2 μ L. The mass scan mode was multiple reaction monitoring mode including positive or negative ion detection modes (Guo et al., 2022).

Liver microsomal Enzyme Activity

Rat liver microsomes from each group were isolated by differential centrifugation as described previously (Modica-Napolitano et al., 2019). The basic incubation system consisted of 50 μ L rat liver microsomes (0.5 mg/mL), 49 μ L NADPH regeneration solution, and 1 μ L cocktail of substrates (6519.5 ng/mL omeprazole, 1686.7 ng/mL metoprolol, 2347.3 ng/mL chlorzoxazone, 667 ng/mL phenacetin, 1250 ng/mL tolbutamide, and 2500 ng/mL midazolam) in a final volume of 100 μ L. The reaction system was incubated at 37°C for various times, and 400 μ L of precooled acetonitrile containing IS was subsequently added to terminate the reaction. The sample was then centrifuged and 100 μ L supernatant was taken for UPLC-MS/MS analysis (Guo et al., 2022).

Western Blotting

The liver samples were lysed with RIPA buffer containing 1 mM PMSF. Total protein was separated by centrifugation and supernatant was taken. The total protein concentration was measured using a BCA assay. Twenty micrograms of total protein were separated on 10% SDS PAGE gels. The isoforms of CYPs protein were detected with the anti-CYP1A2, anti-CYP2C6, anti-CYP2C11, anti-CYP2D1, anti-CYP2E1, and anti-CYP3A1 antibodies, followed by incubation with secondary antibody. Signals were detected using an ECL kit. The relative expression of the target protein was expressed by the gray value ratio of the target protein band to the internal reference protein band.

Quantitation of Serum BAs

Serum bile acid levels were determined by Metabo-Profile, Inc. (Shanghai, China) according to previously reported methods. Forty bile acid standards purchased from Steraloids Inc. (Newport, RI, USA) and TRC Chemicals (Toronto, ON, Canada) were used to quantify serum BAs, and six stable isotope-labeled BAs were bought from C/D/N Isotopes Inc. (Quebec, Canada) and Steraloids (Newport, RI, USA) as IS. Fifty μ L of each serum sample was carefully removed and added to a 1 mL 96-well plate, and then 400 μ L of precooled acetonitrile/methanol (8:2) containing IS was added to extract bile acid metabolites. BAs were quantified by a UPLC-MS/MS (ACQUITY UPLC-Xevo TQ-S, Waters Corp., Milford, MA, USA). Chromatographic separations were performed with an ACQUITY UPLC Cortec's C18 analytical column (2.1 \times 100 mm, 1.6 μ m) and an ACQUITY UPLC Cortec's C18 pre-column (2.1 \times 5.0 mm, 1.6 μ m) (Waters, Milford, MA). The UPLC-MS/MS raw data were analyzed and processed by Masslynx software (Milford, MA).

Statistical Analysis

Significant differences between the wild-type and antibiotics-treated rats were determined using an unpaired Student's *t* test or Mann-Whitney *U* test by IBM SPSS 23.0 software or GraphPad Prism 8.3.0. Except for RNA-Seq statistical analysis, $P < 0.05$ was considered statistically significant in other cases.

Results

Evaluation of Antibiotics-Induced Intestinal Dysbiosis Model

To evaluate whether oral antibiotics deplete rat microbiota, the concentration of 16S ribosomal DNA of fecal bacteria was detected to evaluate the intestinal flora. After 2 weeks of antibiotics treatments, the fecal microbial DNA concentration of rats was significantly reduced by 97%, which could be maintained for 1 week after drug withdrawal, indicating that the extreme model of antibiotics-induced intestinal microbiota depletion was successfully constructed (Fig. 1). At the same time, to evaluate whether high-dose antibiotics caused tissue and organ damage in rats, serum biochemical indexes and pathologic changes in the liver, small intestine, and kidney were detected. As shown in Table 1, compared with wild-type rats, serum albumin and total cholesterol in antibiotics-treated rats were significantly decreased, and other liver function biochemical parameters, such as serum alanine transaminase, aspartate aminotransferase, total bilirubin, alkaline phosphatase, gamma-glutamyl transpeptidase, and triglyceride, as well as renal function indexes, such as blood urea nitrogen, creatinine, and glucose, showed no significant difference between two groups. In addition, H&E staining results showed that antibiotics treatments did not cause obvious tissue injury in the liver, small intestine, and kidney

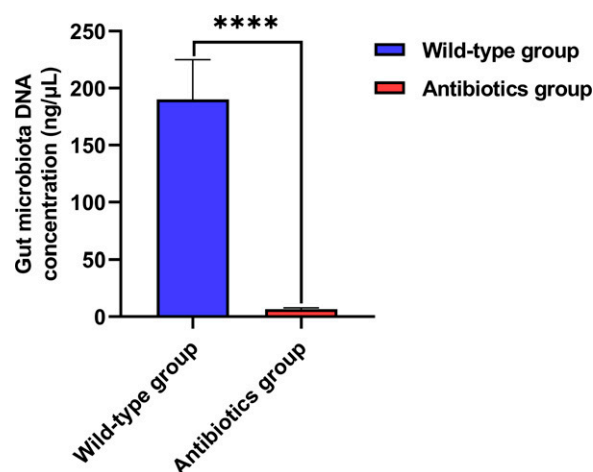


Fig. 1. DNA concentration of rat fecal microbiota after 2 weeks with antibiotics treatments. Data are represented as mean \pm SD, $n = 6$ for each group. **** $P < 0.0001$ vs. wild-type rats.

TABLE 1

Effect of antibiotics treatments on serum biochemical parameters in rats

Parameter	Wild-type rats	Antibiotics-treated rats	P value
ALT (U/L)	168.11 ± 52.80	212.07 ± 87.68	0.55
AST (U/L)	339.74 ± 72.87	358.07 ± 104.19	0.67
TBIL (μmol/L)	19.21 ± 2.53	19.53 ± 4.39	0.85
ALP (U/L)	110.22 ± 31.66	125.81 ± 33.78	0.33
γ-GT (U/L)	3.69 ± 1.07	4.15 ± 1.46	0.46
ALB (g/L)	28.35 ± 1.47	26.62 ± 1.22*	0.02
TC (mmol/L)	2.61 ± 0.20	2.37 ± 0.22*	0.03
TG (mmol/L)	1.35 ± 0.08	1.37 ± 0.13	0.79
BUN (mg/dL)	22.24 ± 1.34	23.38 ± 3.78	0.41
CRE (μmol/L)	26.00 ± 6.05	26.27 ± 6.35	0.93
GLU (mmol/L)	8.21 ± 1.05	7.60 ± 0.66	0.16

ALB, albumin; ALT, serum alanine transaminase; ALP, alkaline phosphatase; AST, aspartate aminotransferase; BUN, blood urea nitrogen; CRE, creatinine; GLU, glucose; TBIL, total bilirubin; TC, total cholesterol; TG, triglyceride; γ-GT, gamma-glutamyl transpeptidase

Data are represented as mean ± SD, n = 9 for each group. *P < 0.05 vs. wild-type rats.

(Supplementary Fig. 1). Therefore, what seems certain is that there is no significant organ toxicity or physiologic change in the extreme model of short-term high-dose antibiotics-induced intestinal microbiota depletion, and the model can be used for subsequent experiments.

Expression Profiles Analysis of Host DPGs

RNA-Seq was used to analyze the effect of antibiotics-induced depletion of rat microbiota on the mRNA expression levels of host

DPGs. Differential expression analysis of liver transcriptome genes showed that antibiotics treatments significantly up-regulated the mRNA expression levels of 26 DPGs and down-regulated 66 DPGs (FDR-BH < 0.05). Differential expression analysis of jejunum transcriptome genes showed that the mRNA expression levels of 35 DPGs were significantly different between the wild-type and antibiotic-treated rats (FDR-BH < 0.05), among which the mRNA expression levels of 8 DPGs were up-regulated and 27 were down-regulated (Table 2).

CYPs are the most important drug-metabolizing enzyme involved in about 90% of the drug metabolism in the market (Jo et al., 2018; Lin et al., 2018; Zhou et al., 2020). Therefore, in this study, the effect of antibiotics treatments on the mRNA expression levels of CYPs in liver and jejunum tissues of rats was compared in detail. As shown in Fig. 2, the mRNA expression levels of *CYP2A1* (36%), *CYP2C11* (90%), *CYP2C13* (54%), *CYP2C23* (47%), *CYP2D2* (43%), *CYP2D3* (33%), *CYP2E1* (66%), *CYP2F4* (51%), *CYP2J4* (60%), *CYP2J10* (32%), *CYP2T1* (62%), *CYP3A18* (66%), *CYP3A23/3A1* (87%), *CYP4B1* (54%), *CYP4F1* (48%), and *CYP4F6* (42%) decreased significantly in the rat liver after antibiotics treatments. On the other hand, antibiotics treatments led to significantly increased levels of *CYP2B2* (309%), *CYP2C7* (154%), and *CYP2C12* (471%) mRNA expression in the rat liver. In the jejunum of antibiotics-treated rats, the mRNA expression levels of *CYP2E1* (93%) and *CYP4F39* (95%) were decreased significantly, while the mRNA expression levels of *CYP1B1* (328%) and *CYP4V3* (188%) were increased significantly. These results indicated

TABLE 2

List of 112 DPGs with differential expression in liver and jejunum of antibiotics-treated rats compared with wild-type rats (FDR-BH < 0.05, Cuffdiff)

DPGs #	Liver		Jejunum	
	Decreased in antibiotics-treated rats (66)	Increased in antibiotics-treated rats (26)	Decreased in antibiotics-treated rats (27)	Increased in antibiotics-treated rats (8)
52 phase I enzymes	8 enzymes involved in hydrolysis reactions	<i>CES1D</i> <i>PON1</i> , 3 <i>EPHX1</i> <i>AADAC</i>	<i>CES1D</i> , 1E, 2C, 2G <i>EPHX1</i> <i>AADAC</i>	
	12 enzymes involved in reduction reactions	<i>AKR7A2</i> , 1C1, 1C2, 1C12, 1C13, 1C19	<i>AKR7A2</i> , 1C19, 1E2 <i>NQO1</i> <i>CBR3</i>	
	22 CYP family	<i>CYB5A</i> , 5R3 <i>CYP2A1</i> , 2C11, 2C13, 2C23, 2D2, 2D3, 2E1, 2F4, 2J4, 2J10, 2T1, 3A18, 3A23/3A1, 4B1, 4F1, 4F6	<i>CYB5B</i> <i>CYP2B2</i> , 2C7, 2C12	<i>CYP2E1</i> , 4F39 <i>CYP1B1</i> , 4V3
	10 non-P450 enzymes	<i>ADH6</i> , <i>FE1</i> <i>ALDH2</i> <i>FMO1</i> , 3 <i>AOX1</i> , 4	<i>ALDH1B1</i> , 1L2 <i>FMO5</i>	<i>ADHFE1</i> <i>ALDH1B1</i> <i>FMO1</i> <i>AOX1</i>
30 phase II enzymes	16 Gsts	<i>GSTA1</i> , A2, A3, A6, K1, M1, M6, M7, O1, P1, T1, T3, Z1	<i>UGT2B10</i>	<i>GSTA3</i> , A5, M4, M6L, O1, P1
	2 Ugts	<i>UGT2B35</i>		
	5 Sults	<i>SULT1A1</i> , 1B1, 1C2, 1C2A, 1E1		
	1 Nat			<i>NAT8L</i>
	3 methyltransferases	<i>INMT</i> , <i>GAMT</i>		<i>TPMT</i>
	3 amino acid conjugation enzymes	<i>ACNAT2</i> , <i>BAAT</i> , <i>GLYAT</i>		
30 transporters	16 uptake	<i>GLUT2</i> , <i>OATP2</i> , <i>MCT4</i> , <i>MCT11</i>	<i>PHT1</i> , <i>GLUT6</i> , <i>OATP3A1</i> , <i>MCT1</i> , <i>TAT1</i> , <i>MCT12</i> , <i>SLC10A5</i> , P7, y+LAT1, <i>CAT2</i>	<i>OCT3</i> <i>GLUT12</i>
	14 efflux	<i>ABCR</i> , <i>SUR</i>	<i>ABCA3</i> , <i>ABCA5</i> , <i>ABCA8</i> , <i>ABCB7</i> , <i>ABCB10</i> , <i>BSEP</i> , <i>MRP4</i> <i>PPARα</i> , <i>RXRα</i>	<i>ABCC10</i> , <i>ABCC50</i> <i>ABC2</i> , <i>MRP1</i> , <i>MRP4</i> , <i>SUR</i> , <i>SUR2</i>
4 TFs		<i>PXR</i>		<i>HNF1α</i>

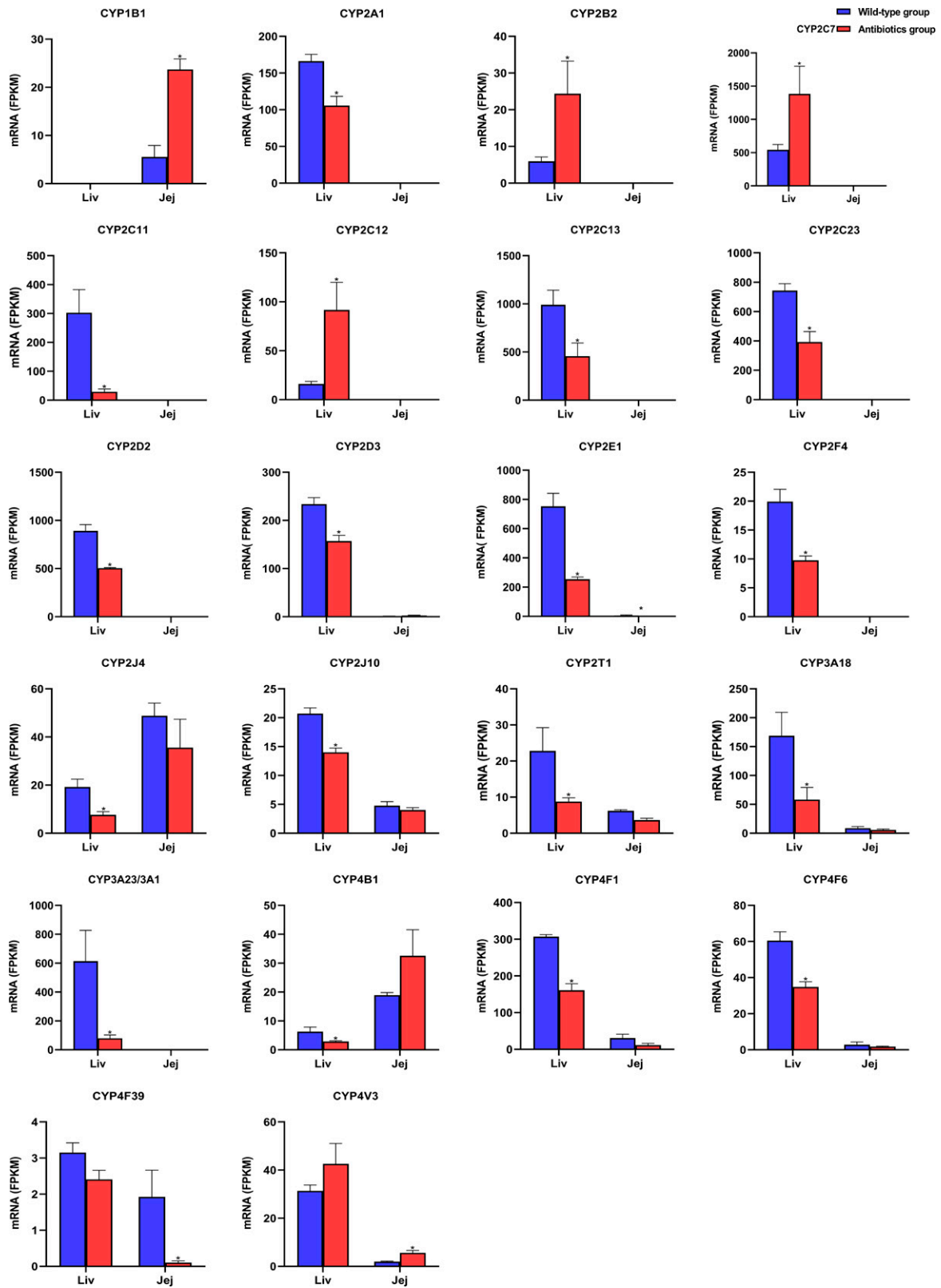


Fig. 2. Effects of microbiota depletion by antibiotics on the mRNA expressions of liver PXR and its target genes in rats. Data are represented as mean FPKM \pm S.E.M., $n = 3$ for each group. * denote statistically significant differences between the wild-type and antibiotics-treated rats (FDR-BH < 0.05, Cuffdiff).

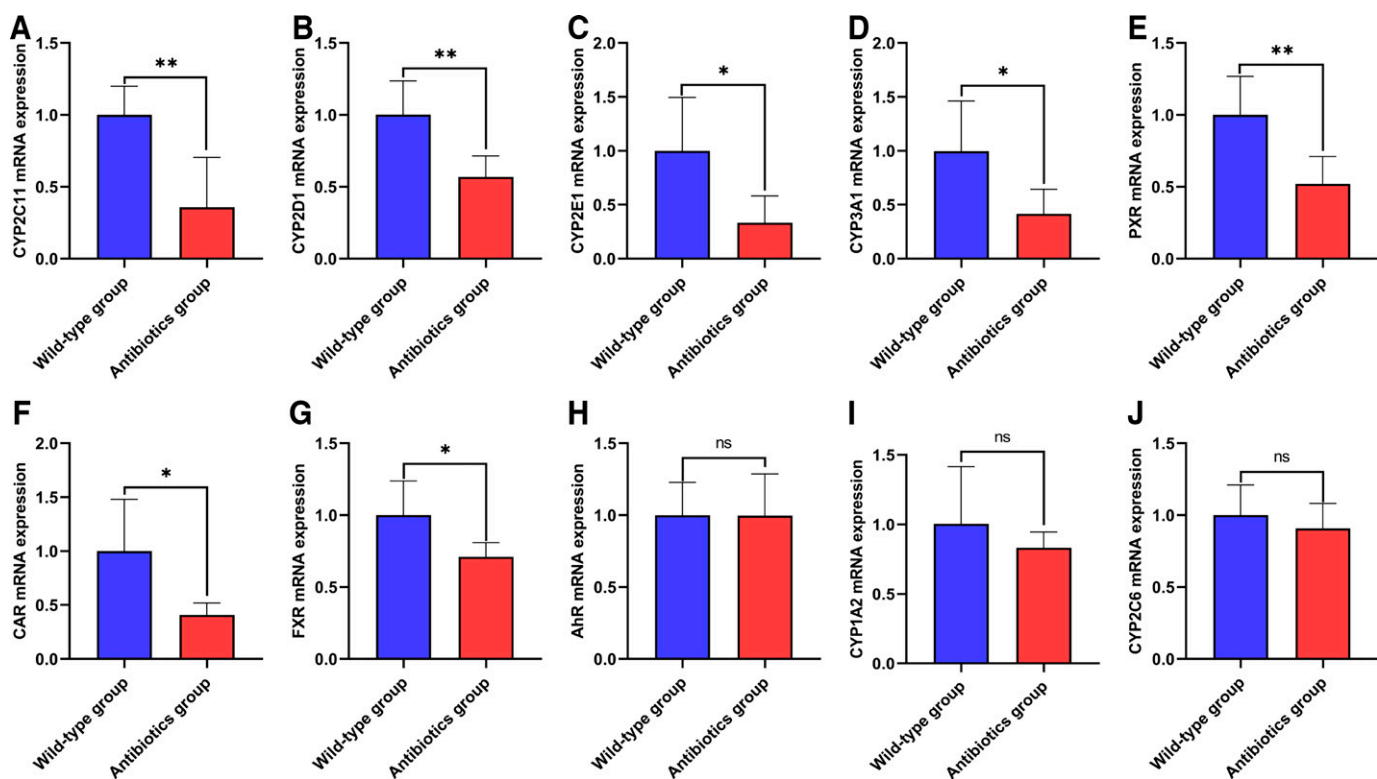


Fig. 3. Expression levels of 10 selected genes validated by RT-qPCR. The relative gene expression was analyzed using the $2^{-\Delta\Delta Ct}$ method and normalized to the expression of the housekeeping genes *GAPDH*. Data are represented as mean \pm SD, $n = 6$ for each group. * $P < 0.05$. ** $P < 0.01$. vs. wild-type rats. ns, no significance.

that the presence of the gut microbiome is essential for maintaining CYPs gene expression.

Validation of Transcriptome Sequencing Results

To validate the reproducibility and repeatability of DPGs identified from the RNA-Seq, we selected 10 of the most important drug-metabolizing enzymes and nuclear receptor genes, namely, *CYP1A2*, *CYP2C6*, *CYP2C11*, *CYP2D1*, *CYP2E1*, *CYP3A1*, *AhR*, *CAR*, *PXR*, and *FXR*, including both genes with and without differential expression shown by RNA-Seq, for RT-qPCR analysis (Fig. 3). The results showed that antibiotics-induced depletion of rat microbiota significantly regulated the expressions of liver *CYP2C11*, *CYP2D1*, *CYP2E1*, *CYP3A1*, *PXR*, *CAR*, and *FXR* at the transcriptional level. Except for *CAR* and *FXR*, other results were consistent with RNA-Seq results. RT-qPCR results showed that the mRNA expressions of *CAR* and *FXR* decreased significantly, while RNA-Seq results showed that the mRNA expressions of *CAR* and *FXR* decreased but did not reach statistical difference, which may be because RNA-Seq selected more stringent differential screening criteria ($FDR-BH < 0.05$). These results further confirmed the reliability of our RNA-Seq results.

Alterations of Pharmacokinetic of CYPs Probe Drugs in Antibiotics-Treated Rats Compared With Wild-Type Rats

Antibiotics-induced depletion of intestinal microbiota resulted in different degrees of changes in the pharmacokinetic parameters of the CYPs probe drugs, such as area under the concentration-time curve (AUC), maximum concentration (C_{max}), eliminate half-life ($t_{1/2}$), time to reach C_{max} (T_{max}), and mean residence time (MRT) (Table 3). The details are given as follows.

Phenacetin. Antibiotics treatments resulted in decreased exposure concentration of phenacetin in rats (Fig. 4A). The $AUC_{(0-24h)}$ and

$AUC_{(0-\infty)}$ significantly decreased (34.2% and 33.9%, respectively) in antibiotics-treated rats compared with wild-type rats (Table 3).

Tolbutamide. The pharmacokinetic (PK) profiles of tolbutamide are shown in Fig. 4B, and the mean PK parameters of tolbutamide, including the $AUC_{(0-24h)}$, $AUC_{(0-\infty)}$, C_{max} , $t_{1/2}$, T_{max} , $MRT_{(0-24h)}$, and $MRT_{(0-\infty)}$, showed no statistically significant differences between the wild-type rats and antibiotics-treated rats (Table 3).

Omeprazole. The PK profiles of omeprazole are shown in Fig. 4C, and the mean PK parameters of omeprazole, the $t_{1/2}$, $MRT_{(0-24h)}$, and $MRT_{(0-\infty)}$ significantly increased (262.1%, 50%, and 56.7%, respectively) in antibiotics-treated rats compared with wild-type rats (Table 3).

Metoprolol. The PK profiles of metoprolol are shown in Fig. 4D, and the mean PK parameters of metoprolol, the $t_{1/2}$, $MRT_{(0-24h)}$, and $MRT_{(0-\infty)}$ significantly increased (208.1%, 45.2%, and 57.1%, respectively) in antibiotics-treated rats compared with wild-type rats (Table 3).

Chlorzoxazone. The exposure concentration of chlorzoxazone in antibiotics-treated rats was lower than that in wild-type rats (Fig. 4E), and the $AUC_{(0-24h)}$, $AUC_{(0-\infty)}$, and C_{max} significantly decreased (49.5%, 49.2%, and 39%, respectively). However, the $t_{1/2}$, $MRT_{(0-24h)}$ and $MRT_{(0-\infty)}$ showed significant increase (276.4%, 33.1%, and 54.3%, respectively) in antibiotics-treated rats compared with wild-type rats (Table 3).

Midazolam. Antibiotics treatments resulted in a significant increase in exposure concentration of midazolam in rats (Fig. 4F), and the $AUC_{(0-24h)}$, $AUC_{(0-\infty)}$, C_{max} , $MRT_{(0-24h)}$, and $MRT_{(0-\infty)}$ significantly increased (156.9%, 160.4%, 193.50%, 30.2%, and 58.2%, respectively) in antibiotics-treated rats compared with wild-type rats (Table 3).

Alterations of Protein Expressions and Activities of Major CYPs in Antibiotics-Treated Rats Compared With Wild-Type Rats

The depletion of intestinal flora induced by antibiotics significantly decreased the protein expression levels of *CYP2E1* and *CYP3A1* in the

TABLE 3
Effects of microbiota depletion by antibiotics on pharmacokinetic parameters of CYPs probe drugs in rats after cocktail administration

Probe drugs	Groups	AUC _(0-24h) (ng/mL·h)	AUC _(0-infinity) (ng/mL·h)	C _{max} (ng/mL)	t _{1/2} (h)	T _{max} (h)	MRT ₍₀₋₂₄₎ (h)	MRT _(0-infinity) (h)
Phenacetin	Wild-type	5,715.88 ± 1,114.75	5,719.10 ± 1,120.80	3,431.67 ± 956.04	2.55 ± 3.01	0.29 ± 0.13	1.30 ± 0.10	1.32 ± 0.10
	Antibiotics	3,761.40 ± 741.10**	3,782.24 ± 747.72**	2,766.67 ± 901.79	8.94 ± 11.90	0.42 ± 0.29	1.25 ± 0.12	1.55 ± 0.50
Tolbutamide	Wild-type	69,547.03 ± 7,922.22	88,474.71 ± 16,660.49	6,625.00 ± 2,238.09	10.51 ± 2.96	0.56 ± 0.28	7.68 ± 0.61	13.16 ± 2.47
	Antibiotics	69,654.76 ± 32,858.88	102,197.27 ± 67,298.70	5,395.00 ± 2,072.80	12.88 ± 7.93	2.29 ± 2.89	8.00 ± 1.35	17.13 ± 12.02
Omeprazole	Wild-type	597.85 ± 130.64	599.44 ± 131.23	644.00 ± 156.24	0.66 ± 0.33	0.28 ± 0.14	0.86 ± 0.26	0.90 ± 0.27
	Antibiotics	516.90 ± 244.72	518.13 ± 244.54	548.33 ± 317.73	2.39 ± 2.35*	0.42 ± 0.29	1.29 ± 0.39*	1.41 ± 0.43*
Metoprolol	Wild-type	210.80 ± 59.54	211.38 ± 58.49	168.23 ± 70.29	1.36 ± 0.14	0.51 ± 0.73	1.97 ± 0.13	2.03 ± 0.17
	Antibiotics	231.55 ± 103.95	233.43 ± 102.84	174.80 ± 142.15	4.19 ± 2.05**	0.38 ± 0.32	2.86 ± 0.77*	3.19 ± 0.98*
Chlorzoxazone	Wild-type	1,320.55 ± 312.22	1,320.55 ± 312.22	1,223.00 ± 362.87	1.06 ± 0.11	0.25 ± 0.07	1.60 ± 0.17	1.64 ± 0.17
	Antibiotics	666.69 ± 163.93**	670.94 ± 167.61**	746.00 ± 253.23*	3.99 ± 2.21**	0.24 ± 0.08	2.13 ± 0.65*	2.53 ± 0.76*
Midazolam	Wild-type	53.87 ± 14.76	53.98 ± 14.75	41.27 ± 15.01	1.70 ± 0.54	0.21 ± 0.07	1.82 ± 0.27	1.84 ± 0.26
	Antibiotics	138.40 ± 24.31****	140.55 ± 24.69****	121.13 ± 18.98****	4.82 ± 3.44	0.24 ± 0.06	2.37 ± 0.48*	2.91 ± 0.97*

Data are represented as mean ± SD, n = 6 for each group. *P < 0.05, **P < 0.01, ****P < 0.0001 vs. wild-type rats.

liver by 43.25% and 70.47%, respectively (Fig. 5). At the same time, the enzymatic activity levels of *CYP2D1*, *CYP2E1*, and *CYP3A1* in antibiotics-treated rats were significantly reduced by 40.52%, 50.56%, and 59.27%, respectively (Fig. 6). Results showed that the host *CYP2E1* and *CYP3A1* activities and expressions may be regulated by the absence of gut microflora.

Alterations of Serum BA Profiles in Antibiotics-Treated Rats Compared With Wild-Type Rats

UPLC-MS/MS was used to detect the absolute contents of 42 BAs in rat serum. Unidimensional statistical analysis was used to analyze the effect of antibiotics-induced depletion of gut microbiota on the composition of the serum bile acid pool of rats. Results showed that antibiotics treatments significantly changed the serum levels of 28 BAs in rats, of which 15 were up-regulated (α MCA, β MCA, CA, UDCA, CDCA, GCA, GCDCA, UCA, AlloCA, NorCA, 7-KetoLCA, apoCA, 7-DHCA, 12-DHCA, and 3-DHCA) and 13 were down-regulated (ω MCA, muroCA, β HDCA, HDCA, β DCA, isoLCA, LCA, 6-KetoLCA, 12-KetoLCA, T ω MCA, THDCA, TDCA, and TLCA) (Table 4). Classification and

statistical analysis of 42 kinds of BAs showed that, compared with the wild-type rats, serum total BAs increased by 83.07%, total primary BAs increased by 1.75 times, total secondary BAs decreased by 56.8%, the ratio of total secondary BAs to primary BAs significantly decreased, the unconjugated BAs increased by 2.80 times, and the ratio of conjugated BAs to unconjugated BAs decreased significantly in antibiotics-treated rats. In addition, glycine-conjugated BAs increased by 1.41 times, and the ratio of taurine-conjugated BAs to glycine-conjugated BAs decreased significantly in antibiotics-treated rats compared with wild-type rats (Fig. 7).

The mRNA Expression Levels of Liver *PXR* and Its Target Genes Were Decreased in Antibiotics-Treated Rats

Lithocholic acid (LCA), a secondary bile acid produced only by the gut microbiota, is a strong ligand of *PXR* (Staudinger et al., 2001; Jurica et al., 2016), and serum LCA was significantly reduced in antibiotics-treated rats (Table 4). Therefore, in this study, combined with transcriptome sequencing results, the mRNA expression levels of *PXR* and its target genes in liver were further analyzed. The mRNA expression level

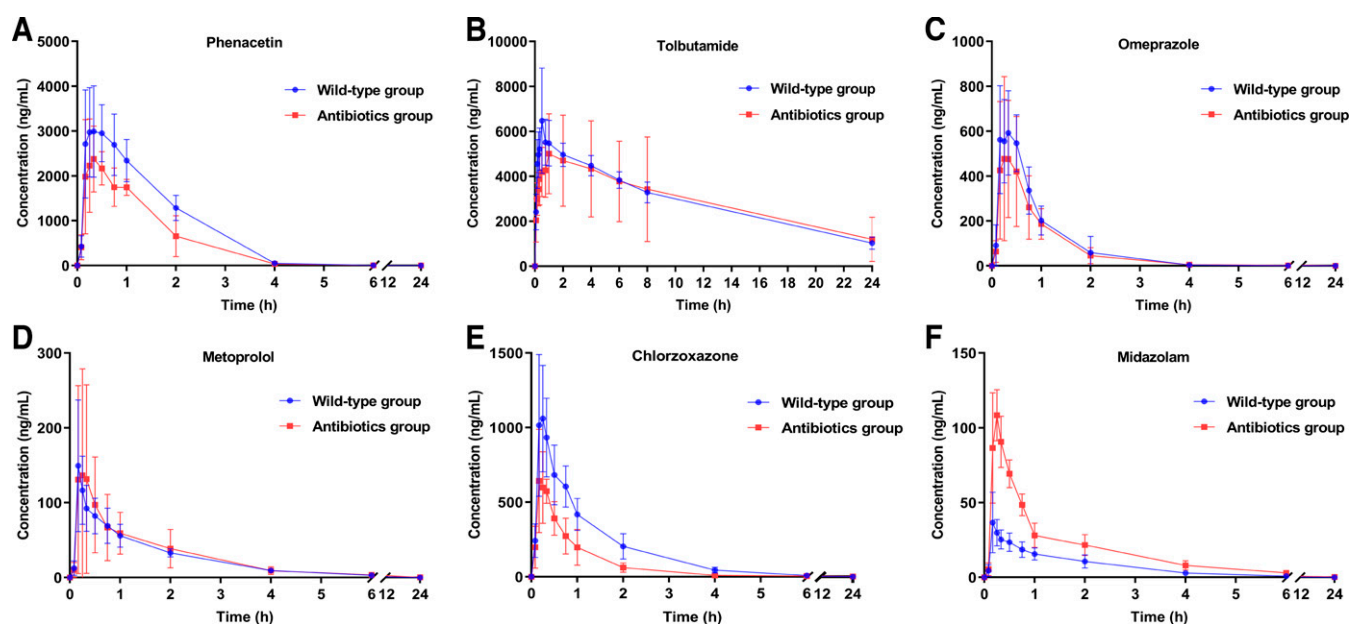


Fig. 4. Effects of microbiota depletion by antibiotics on mean plasma concentration-time curves of CYPs probe drugs in rats after cocktail administration. (A) Phenacetin, (B) tolbutamide, (C) omeprazole, (D) metoprolol, (E) chlorzoxazone, and (F) midazolam. Data are represented as mean ± SD, n = 6 for each group.

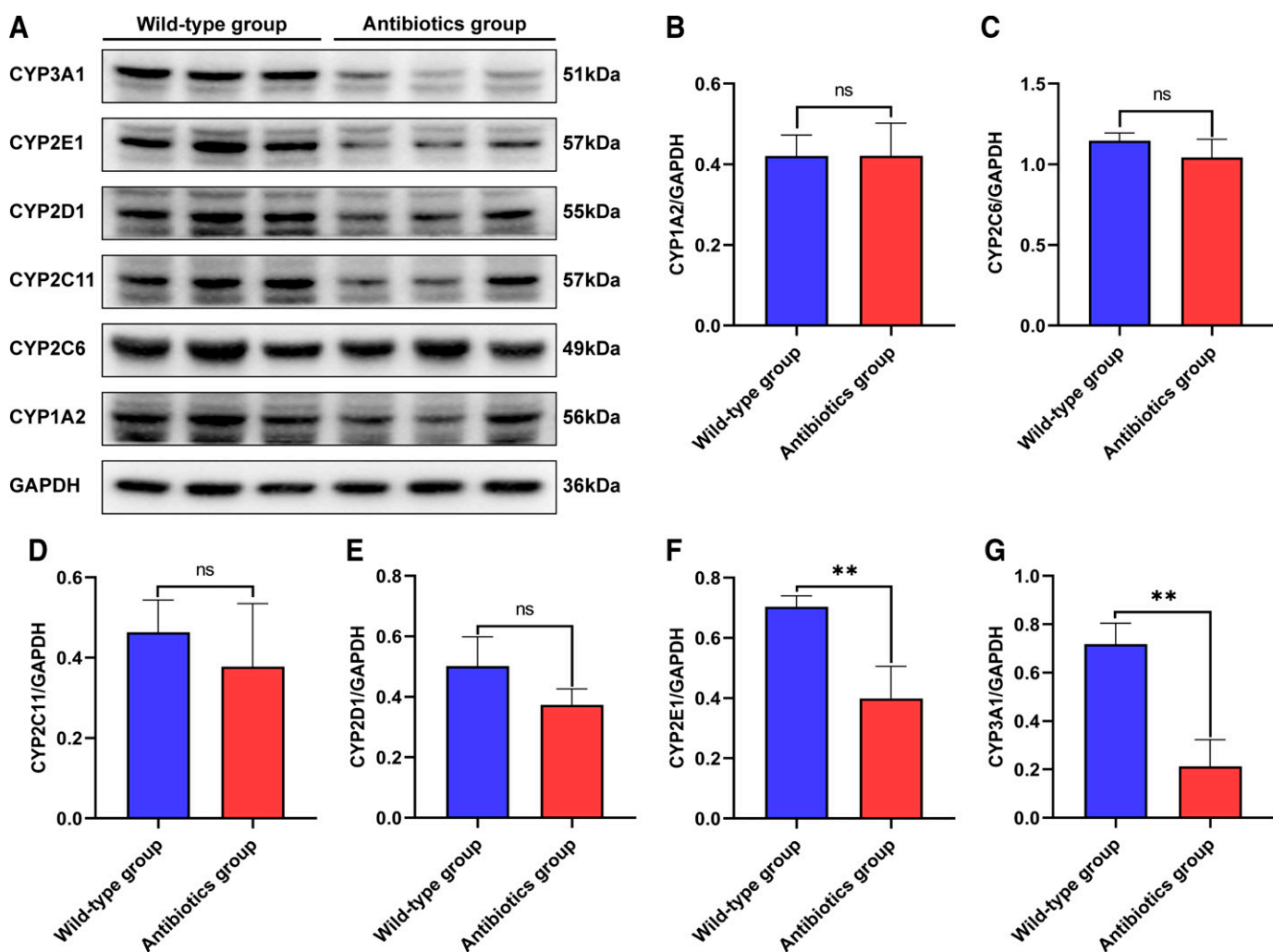


Fig. 5. Effects of microbiota depletion by antibiotics on the protein expressions of major CYPs in rat liver. (A) Protein expressions of host major CYP enzymes in the liver were assessed by western blotting. *GAPDH* was used as the loading control for western blotting. (B–G) Densitometry analysis of western blotting results on major CYPs. Data are represented as mean \pm SD, $n = 3$ for each group. ** $P < 0.01$ vs. wild-type rats. ns, no significance.

of *PXR* significantly decreased by 48%. The mRNA expression levels of *PXR*-targeted DPGs *CYP3A1*, *CYP3A18*, *OATP2*, *GSTA2*, *GSTM1*, and *GSTT3* significantly decreased by 87%, 66%, 72%, 85%, 63%, and 45%, respectively (Fig. 8). The significant decrease in mRNA expression levels of *PXR* and its target genes may be attributed to the reduction of serum LCA caused by antibiotics-induced intestinal microbiota depletion, which leads to the inactivation of the *PXR* signaling pathway.

Discussion

Variation of DPGs are considered to be the basis of individual differences in drug response. In the present study, we found that the depletion of rat microbiota by antibiotics treatments significantly altered the mRNA expression levels of 112 DPGs in liver and jejunum tissues (Table 2) and affected the pharmacokinetic characteristics of CYPs probe drugs (Table 3; Fig. 4).

Four studies have previously illustrated changes in mRNA expressions of DPGs in liver or intestinal tissue of GF and conventional mice (Björkholm et al., 2009; Toda et al., 2009b; Selwyn et al., 2015; Fu et al., 2017). Combined with our experimental results, comprehensive comparison showed that the mRNA expression changes of DPGs in three strains of C57BL6 GF mice, NMRI GF mice, and IQI GF mice

were completely inconsistent with those of corresponding wild-type mice of the same strain. In addition, the results observed in antibiotics-treated rats were also partially different from their reports. Since the gene homology of DPGs in rats and mice cannot be completely one to one, we focus discussion on a group of CYPs genes involved in more than 90% of clinical drug metabolism, namely *CYP1A2*, *CYP2C6*, *CYP2C11*, *CYP2D1*, *CYP2E1*, and *CYP3A1*.

Human *CYP3A4* is an important drug metabolism enzyme, which can metabolize more than 50% of the drugs on the market (Zuber et al., 2002). Consistent with previous studies, in our results, the mRNA level of *CYP3A1*, a rat homolog of human *CYP3A4* (Martignoni et al., 2006), in the liver of antibiotics-treated rats was significantly reduced (87%) compared with wild-type rats (Fig. 2B). Meanwhile, antibiotics treatments also significantly decreased *CYP3A1* protein expression and enzyme activity in rats (Fig. 5G; Fig. 6F). In addition, pharmacokinetic studies showed that the AUC, C_{max} , and MRT of midazolam in antibiotics-treated rats were higher than those in wild-type rats (Table 3). These results suggested that intestinal flora can regulate the expression of *CYP3A4* in the human liver, thus affecting the pharmacokinetic behavior of drug metabolism by this enzyme.

It is noteworthy that antibiotics treatments significantly decreased the expression and enzyme activity of *CYP2E1* in rat liver (Fig. 2B,

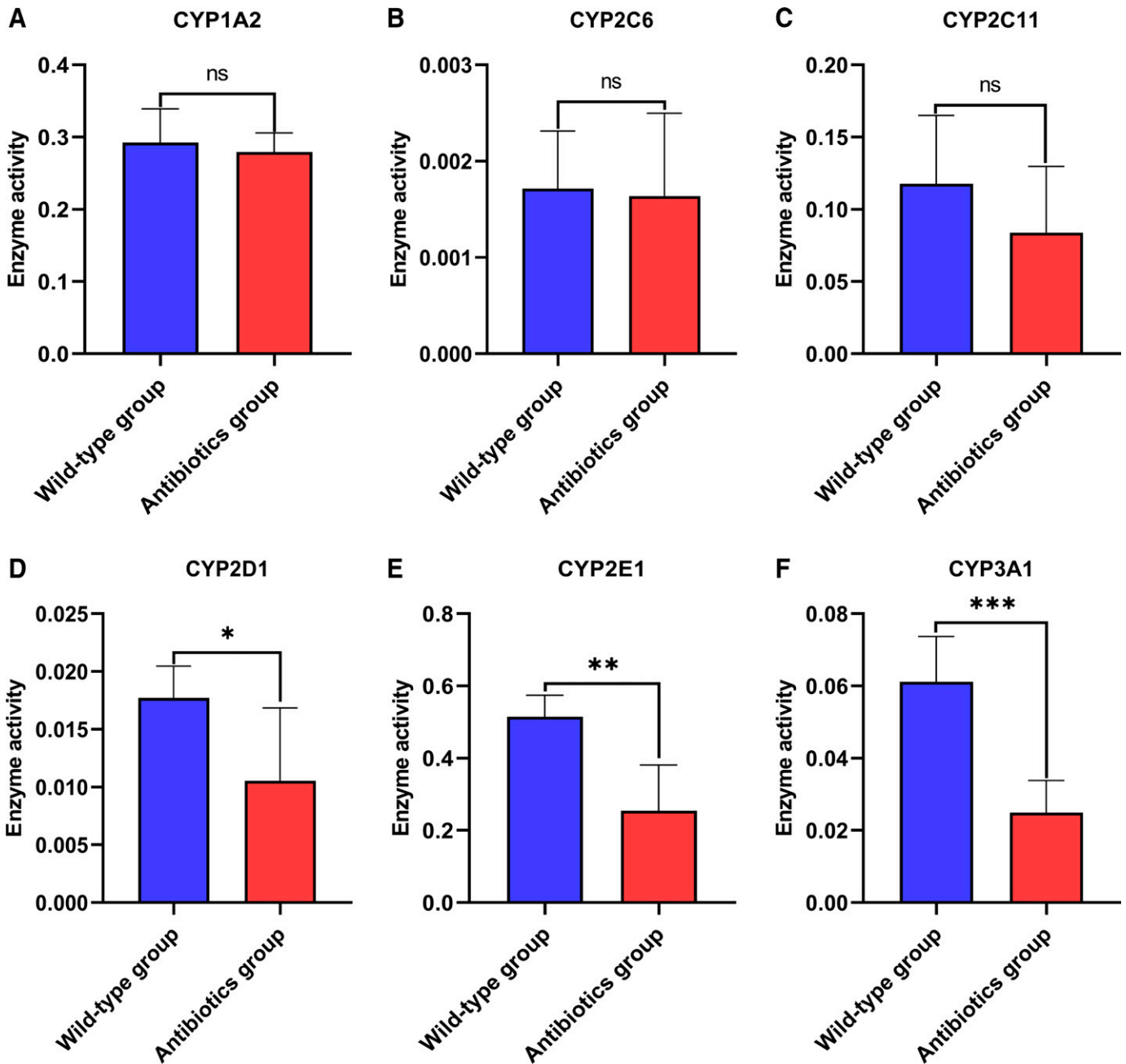


Fig. 6. Effects of microbiota depletion by antibiotics on the enzymatic activities of major CYPs in rat liver. (A–F) Major CYPs enzymatic activities were measured in the liver microsomes. Data are represented as mean \pm SD, $n = 5$ for each group. * $P < 0.05$. ** $P < 0.01$. *** $P < 0.001$ vs. wild-type rats. ns, no significance.

Fig. 5F, and Fig. 6E). Previous studies have shown that *Cyp2e1* mRNA expression levels are significantly increased in GF mice (Fu et al., 2017; Jourová et al., 2017). The reasons for the difference in results between antibiotics-treated rats and GF mice may be the different animal strains or the potential impact of high-dose antibiotics modeling, which needs further investigation. In addition, this study also investigated the pharmacokinetic changes of chlorzoxazone metabolized by *CYP2E1*. Compared with wild-type rats, the $t_{1/2}$ and MRT of chlorzoxazone showed a significant increase in the antibiotics-treated rats, indicating that drug metabolism in vivo was slowed and drug residence time in vivo was prolonged, which may be caused by decreased *CYP2E1* activity in liver (Table 3). Besides, studies have shown that *Cyp1a2* increased at the mRNA level but decreased at the protein level in GF

mice (Selwyn et al., 2015; Kuno et al., 2016), whereas in our study, there was no statistical difference in the expression and activity of *CYP1A2* between antibiotics-treated rats and wild-type rats (Fig. 5B; Fig. 6A), indicating that GF conditions and antibiotics treatments had different effects on host drug-metabolizing enzymes. In pharmacomicrobiome studies, therefore, we believe that at least some degree of reproducibility should be assessed for the results of studies in GF and antibiotics-treated mice to exclude developmental differences or potential off-target drug effects, which would be of high value in determining the conclusions of most studies.

CYP2C6 is the rat homologous gene of human *CYP2C9*, *CYP2C11* is the rat homologous gene of human *CYP2C19*, and *CYP2D1* is the rat homologous gene of human *CYP2D6* (Martignoni et al., 2006).

TABLE 4
Serum concentrations of 42 BAs are affected by antibiotics in rats

Bile acids (nmol/L)	Wild-type rats	Antibiotics-treated rats	Change
α MCA ^b	77.04 [19.45, 151.92]	999.51 [402.25, 2105.73] **	↑
β MCA ^b	175.13 [56.82, 240.82]	536.34 [308.59, 732.21] **	↑
CA ^b	682.60 [380.61, 917.13]	3877.39 [2288.80, 6665.40] **	↑
UDCA ^b	1.98 [1.23, 2.36]	121.00 [62.52, 220.27] ***	↑
CDCA ^b	66.76 [17.65, 83.00]	715.09 [347.72, 1686.15] ***	↑
T α MCA ^b	173.91 [149.11, 255.03]	149.51 [124.89, 258.34]	–
T β MCA ^b	98.97 [76.15, 169.84]	41.91 [36.05, 103.36]	–
TCA ^b	730.05 [664.34, 1197.21]	628.40 [369.17, 746.06]	–
TUDCA ^b	2.28 [1.95, 4.45]	2.12 [1.78, 4.79]	–
TCDCa ^b	127.73 [119.99, 159.46]	134.32 [110.57, 182.87]	–
GCA ^b	185.25 [79.99, 228.13]	310.84 [233.61, 446.51] *	↑
GUDCA ^b	0.17 [0.03, 0.45]	3.20 [0.44, 4.47]	–
GCDCA ^b	7.69 [4.40, 14.82]	82.03 [46.70, 118.83] **	↑
UCA ^b	0.40 [0.03, 2.85]	18.27 [13.97, 77.34] **	↑
ω MCA ^b	46.23 [20.29, 95.70]	1.89 [1.89, 1.89] **	↓
HCA ^b	0.96 [0.63, 2.56]	3.92 [1.69, 12.36]	–
AlloCA ^b	15.67 [10.99, 29.37]	114.77 [28.90, 184.49] *	↑
NorCA ^b	0.33 [0.33, 0.33]	4.31 [3.51, 4.87] ***	↑
muroCA ^b	58.52 [31.31, 88.23]	9.24 [7.64, 12.36] ***	↓
β UDCA ^b	2.20 [1.94, 2.79]	2.21 [1.65, 2.53]	–
β HDCA ^b	121.91 [70.58, 168.55]	1.25 [0.23, 8.63] ***	↓
HDCA ^b	624.21 [349.90, 825.80]	0.08 [0.08, 0.27] ***	↓
β DCa ^b	22.75 [16.98, 31.69]	7.34 [6.45, 9.74] **	↓
DCA ^a	119.81 [95.28, 192.12]	79.12 [30.84, 127.20]	–
isoLCA ^b	1.93 [1.50, 3.54]	0.20 [0.10, 0.30] ***	↓
LCA ^b	8.06 [6.34, 12.86]	0.79 [0.01, 2.37] **	↓
LCA-3S ^b	1.12 [1.10, 1.46]	1.10 [1.04, 1.16]	–
6-KetoLCA ^b	43.04 [29.84, 55.56]	2.29 [1.08, 3.92] ***	↓
7-KetoLCA ^b	0.38 [0.13, 1.55]	21.50 [10.66, 43.08] **	↑
12-KetoLCA ^b	15.45 [12.55, 16.91]	2.12 [0.23, 3.40] **	↓
apoCA ^b	3.51 [1.93, 8.03]	23.12 [13.02, 33.73] *	↑
6, 7-DiketoLCA ^b	2.77 [1.24, 4.26]	2.81 [2.20, 6.06]	–
DHCA ^b	3.43 [2.70, 3.98]	4.81 [3.26, 6.70]	–
7-DHCA ^b	8.49 [4.59, 16.03]	64.11 [47.59, 251.92] *	↑
12-DHCA ^b	18.70 [8.34, 25.48]	263.08 [148.71, 608.49] **	↑
3-DHCA ^b	6.89 [5.42, 9.70]	51.57 [24.77, 65.68] **	↑
ToMCA ^b	20.84 [18.57, 39.05]	4.09 [3.20, 4.56] ***	↓
THDCA ^b	667.61 [571.38, 1009.61]	5.04 [4.83, 5.32] **	↓
TDCA ^b	62.80 [45.33, 105.03]	8.97 [5.63, 18.23] **	↓
TDHCA ^b	2.30 [2.29, 2.32]	2.28 [2.28, 2.31]	–
TLCA ^b	4.48 [4.40, 4.56]	4.28 [0.43, 4.29] **	↓
GDCa ^b	0.24 [0.03, 7.65]	1.35 [0.03, 10.35]	–

↑, significantly increased; ↓, significantly decreased; –, not significant.

^a One-way ANOVA was used to compare differences between the wild-type rats vs. antibiotics-treated rats.

^b Mann-Whitney *U* test was used to compare differences between the wild-type rats vs. antibiotics-treated rats.

Data are present as median (Q1, Q3), n = 8 for each group. **P* < 0.05. ***P* < 0.01. ****P* < 0.001 vs. wild-type rats.

Antibiotics treatments had no effect on the expression and activity of *CYP2C6* in rats. In addition, compared with wild-type rats, the mRNA expressions of *CYP2C11* and *CYP2D1* in the liver of antibiotics-treated rats were significantly decreased (Fig. 2A), and the enzyme activity of *CYP2D1* was significantly down-regulated (Fig. 6D), but there was no statistical difference in protein expression between the two groups (Fig. 5, D and E). This also indicated that changes in mRNA levels do not necessarily lead to corresponding changes in protein function and activity. Due to technical limitations, only six main protein expressions and enzyme activities of CYPs subtypes were detected in this study. Technological breakthroughs in proteomics and metabolomics have been critical in determining the protein expression levels and activities of those differentially expressed DPGs.

Previous studies have shown that microbial metabolites, such as BAs, regulate the expression of host DPGs through the xenobiotic-sensing transcription factors, such as *FXR*, *PXR*, *CAR*, and *AhR*. Studies have shown that the mRNA expression level of *Cyp3a11* increased in the liver of GF mice after lithocholic acid (LCA) administration (Toda et al., 2009a). LCA, a secondary bile acid produced only by gut microflora, is a potent ligand for *FXR* and *PXR* (Toda et al., 2009b; Juřica

et al., 2016). In our experiment, antibiotics treatments resulted in a significant decrease in liver *PXR* mRNA expression (Fig. 8), which was consistent with the previously reported decrease in *PXR* mRNA expression in GF mice (Toda et al., 2009b). In addition, the DPGs expression profiles of liver *PXR* target genes were also compared between wild-type rats and antibiotics-treated rats. Antibiotics treatments in rat resulted in significantly decreased levels of liver *PXR* target genes *CYP3A1*, *CYP3A18*, *OATP2*, *GSTA2*, *GSTM1*, and *GSTT3* mRNA expression (Fig. 8). Therefore, the expressive suppression of *PXR* and its target and genes may result from the reduction of LCA due to the absence of intestinal flora.

In recent years, many researchers have investigated the effects of gut microbiota on dietary compounds or phytochemicals pharmacokinetics in GF mice, whereas studies on conventional or prescription drugs are limited (Kim, 2015; Yip and Chan, 2015; Choi et al., 2018). This study investigated the effects of antibiotics-induced depletion of rat microbiota on the pharmacokinetic behaviors of six probe drugs: phenacetin, tolbutamide, omeprazole, metoprolol, chlorzoxazone, and midazolam. Cocktail administration is more efficient than single drug administration, which can save the number of animals and cost and can provide more

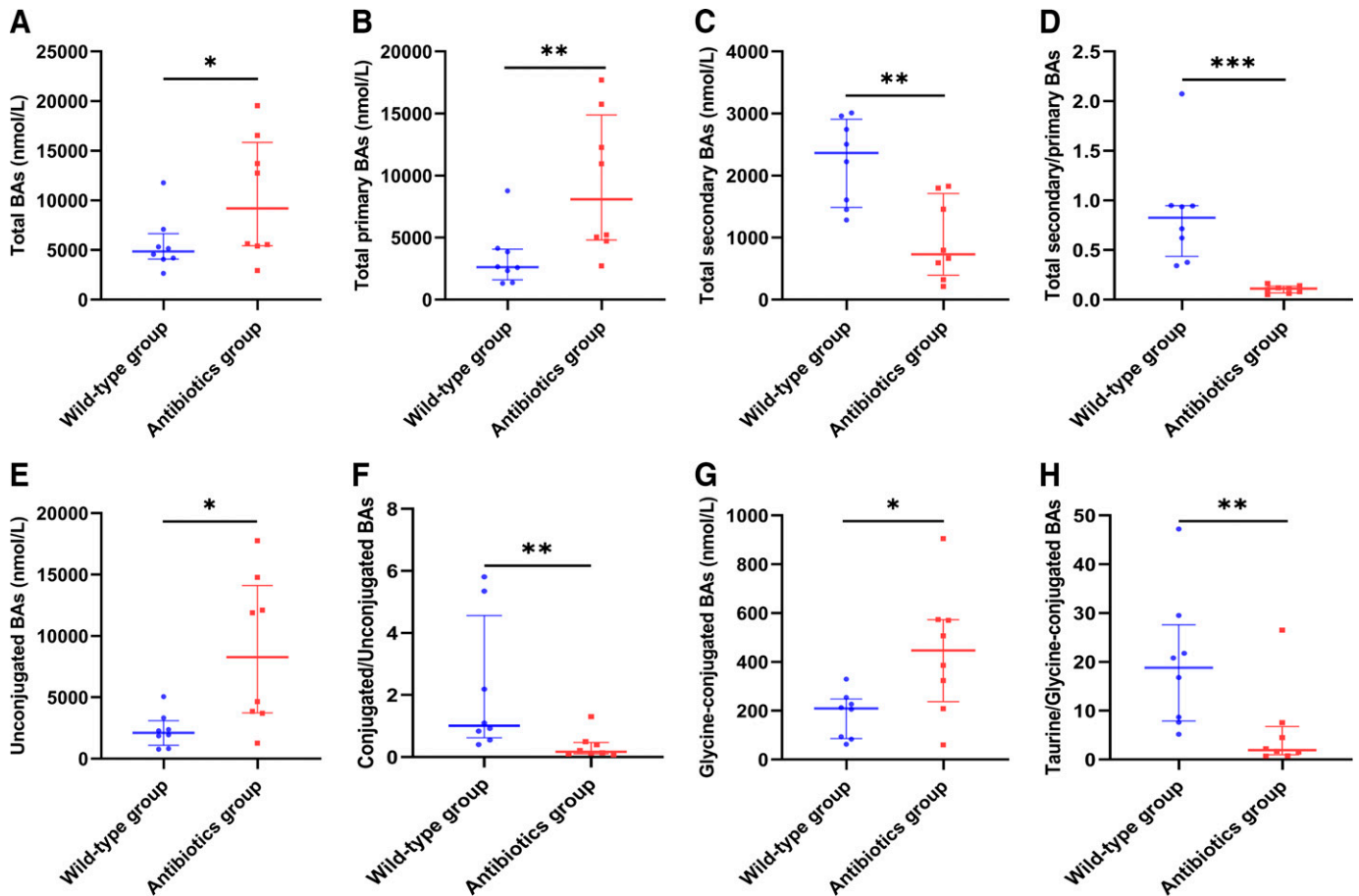


Fig. 7. Analysis of serum BAs composition in wild-type rats and antibiotics-treated rats. (A) Total concentrations of the 42 detected Bas. (B) Total primary BAs (α MCA, β MCA, CA, UDCA, CDCA, T α MCA, T β MCA, TCA, TUDCA, TCDCA, GCA, GUDCA, and GCDCA). (C) Total secondary BAs (UCA, ω MCA, HCA, Al-loCA, NorCA, muroCA, β UDCA, β HDCA, HDCA, β DCA, DCA, isoLCA, LCA, LCA-3S, 6-KetoLCA, 7-KetoLCA, 12-KetoLCA, apoCA, 6,7-DiketolCA, DHCA, 7-DHCA, 12-DHCA, 3-DHCA, T ω MCA, THDCA, TDCA, TDHCA, TLCA, and GDCA). (D) Ratio of total secondary to primary BAs. (E) Unconjugated BAs. (F) Ratio of conjugated to unconjugated BAs. (G) Glycine-conjugated BAs. (H) Ratio of Taurine-conjugated to glycine-conjugated BAs. Data are present as median (Q1, Q3), n = 8 for each group. * $P < 0.05$. ** $P < 0.01$. *** $P < 0.001$ vs. wild-type rats.

pharmacokinetic information from the same experimental process. This study showed that the pharmacokinetic behaviors of probe drugs in rats showed three trends after antibiotics treatments. First, metabolism slowed down and drug concentration increased in the body, which may lead to improved drug efficacy or increase the risk of adverse drug reactions. Antibiotics treatments increased the AUC of midazolam by 156.9%, increased C_{max} by 193.50%, and slowed down metabolism and prolonged MRT in rats. The pharmacokinetic changes of midazolam were mainly affected by antibiotics treatments on the expression of

drug-metabolizing enzyme *CYP3A1*, which was consistent with previous studies (Togao et al., 2020). Second, the reduction of absorption and drug exposure may lead to the reduction of drug efficacy or ineffectiveness. The AUC of phenacetin decreased by 34.2%, and the AUC and C_{max} of chlorzoxazone decreased by 49.5% and 39%, respectively, indicating that antibiotics treatments significantly affected the intestinal absorption of phenacetin and chlorzoxazone in rats. Third, the depletion of gut microbiota did not affect the pharmacokinetic behavior of tolbutamide under antibiotics treatments in this study. It has been reported

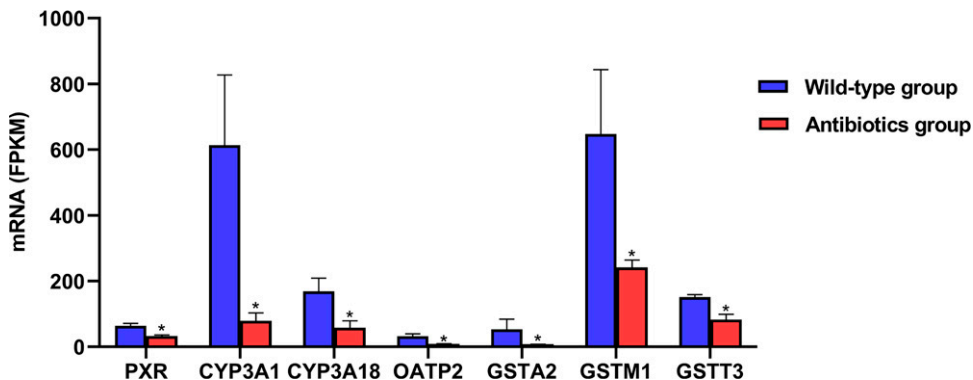


Fig. 8. Effects of microbiota depletion by antibiotics on the mRNA expressions of liver *PXR* and its target genes in rats. Data are represented as mean FPKM \pm S.E.M., n = 3 for each group. denote statistically significant differences between the wild-type and antibiotics-treated rats (FDR-BH < 0.05 , Cuffdiff).

that the deconjugation of the bile acid steroidal core regulated by the microbial enzymes' bile salt hydrolase and the extent of bile acid hydroxylation regulated by microbial 7α -dehydroxylase affect the solubilization capacity of bile salt micelles of insoluble drugs (Enright et al., 2017). In this study, it was found that the serum conjugated BAs and secondary BAs contents of antibiotics-treated rats were significantly reduced (Fig. 8, C, D, and F), which may lead to the decreased ability of intestinal bile salt micelles to dissolve insoluble drugs such as phenacetin, omeprazole, metoprolol, and chlorzoxazone, resulting in reduced intestinal drug absorption. These results suggested that the intestinal absorption of drugs was affected after the depletion of intestinal flora. Therefore, it is necessary to further study the effects of antibiotics-induced depletion of rat intestinal microbiota on the in vivo processes of the six probe drugs after intravenous administration and take both results into account to determine the effects of antibiotics treatments on pharmacokinetic behaviors.

In summary, the absence of gut microflora, whether under GF conditions or antibiotics-induced intestinal dysbiosis conditions, alters the expression of a lot of host DPGs and affects the pharmacokinetic characteristics of probe drugs. Although these conclusions are carried out on the intestinal flora's extreme manipulation, in the context of the current abuse of antibiotics, probiotics, and prebiotics, it is of great guiding value to extensively explore individual differences in the pharmacokinetics of clinically common drugs from a metagenomic perspective. In the future, careful manipulation of the gut microbiota in the future may open up unprecedented opportunities for personalized medicine.

Acknowledgments

The authors thank Yicheng Wang and Kang He from the Drug Analysis Center of Xiangya Hospital, Central South University, for their help with UPLC-MS/MS technique.

Authorship Contributions

Participated in research design: H. Zhou, W. Zhang, Shu, X. Li, Q. Li.

Conducted experiments: Yang, Y. Zhang.

Performed data analysis: Yang, R. Zhou.

Wrote or contributed to the writing of the manuscript: Yang, R. Zhou, Wu, Zhu, Liu, J. Zhou, Yalan Xiong, Yanling Xiong.

References

- Björkholm B, Bok CM, Lundin A, Rafter J, Hibberd ML, and Pettersson S (2009) Intestinal microbiota regulate xenobiotic metabolism in the liver. *PLoS One* **4**:e6958.
- Choi MS, Yu JS, Yoo HH, and Kim DH (2018) The role of gut microbiota in the pharmacokinetics of antihypertensive drugs. *Pharmacol Res* **130**:164–171.
- Claus SP, Ellero SL, Berger B, Krause L, Bruttin A, Molina J, Paris A, Want EJ, de Waziers I, Cloarec O et al. (2011) Colonization-induced host-gut microbial metabolic interaction. *MBio* **2**:e00271–10.
- Enright EF, Joyce SA, Gahan CG, and Griffin BT (2017) Impact of gut microbiota-mediated bile acid metabolism on the solubilization capacity of bile salt micelles and drug solubility. *Mol Pharm* **14**:1251–1263.
- Fu ZD, Selwyn FP, Cui JY, and Klaassen CD (2017) RNA-Seq profiling of intestinal expression of xenobiotic processing genes in germ-free mice. *Drug Metab Dispos* **45**:1225–1238.
- Guo J, Xu Y, Chen L-j, Zhang S-x, Liou Y-l, Chen X-p, Tan Z-r, Zhou H-h, Zhang W, and Chen Y (2022) Gut microbiota and host Cyp450s co-contribute to pharmacokinetic variability in mice with non-alcoholic steatohepatitis: effects vary from drug to drug. *J Adv Res* **39**:319–332.
- Guo YP, Shao L, Chen MY, Qiao RF, Zhang W, Yuan JB, and Huang WH (2020) In vivo metabolic profiles of *Panax notoginseng* saponins mediated by gut microbiota in rats. *J Agric Food Chem* **68**:6835–6844.
- Haiser HJ, Gootenberg DB, Chatman K, Sirasani G, Balskus EP, and Turnbaugh PJ (2013) Predicting and manipulating cardiac drug inactivation by the human gut bacterium *Eggerthella lenta*. *Science* **341**:295–298.
- Huang Y, Zheng SL, Xu ZS, and Hou Y (2014) Effects of *Alismatis rhizome* on rat cytochrome P450 enzymes. *Pharm Biol* **52**:681–687.
- Jernberg C, Löfmark S, Edlund C, and Jansson JK (2010) Long-term impacts of antibiotic exposure on the human intestinal microbiota. *Microbiology (Reading)* **156**:3216–3223.

- Jing B, Zhang C, Liu X, Zhou L, Liu J, Yao Y, Yu J, Weng Y, Pan M, Liu J et al. (2018) Glycosylation of dentin matrix protein 1 is a novel key element for astrocyte maturation and BBB integrity. *Protein Cell* **9**:298–309.
- Jo JJ, Jo JH, Kim S, Lee JM, and Lee S (2018) Development of a simultaneous LC-MS/MS method to predict in vivo drug-drug interaction in mice. *Arch Pharm Res* **41**:450–458.
- Jourová L, Anzenbacher P, Lišková B, Matušková Z, Hermanová P, Hudcovic T, Kozáková H, Hrnčířová L, and Anzenbacherová E (2017) Colonization by non-pathogenic bacteria alters mRNA expression of cytochromes P450 in originally germ-free mice. *Folia Microbiol (Praha)* **62**:463–469.
- Juriča J, Dovrtělová G, Nosková K, and Zendluka O (2016) Bile acids, nuclear receptors and cytochrome P450. *Physiol Res* **65** (Suppl 4):S427–S440.
- Kennedy EA, King KY, and Baldrige MT (2018) Mouse microbiota models: comparing germ-free mice and antibiotics treatment as tools for modifying gut bacteria. *Front Physiol* **9**:1534.
- Kim DH (2015) Gut microbiota-mediated drug-antibiotic interactions. *Drug Metab Dispos* **43**:1581–1589.
- Koppel N, Maini Rekdal V, and Balskus EP (2017) Chemical transformation of xenobiotics by the human gut microbiota. *Science* **356**:eaag2770.
- Kuno T, Hirayama-Kurogi M, Ito S, and Ohtsuki S (2016) Effect of intestinal flora on protein expression of drug-metabolizing enzymes and transporters in the liver and kidney of germ-free and antibiotics-treated mice. *Mol Pharm* **13**:2691–2701.
- Lin Y, Wei Y, Hu X, Wu M, Ying X, and Ding M (2018) Influences of *Oldenlandia diffusa* on the CYP450 activities in rats using a cocktail method by UHPLC-MS/MS. *Biochem Res Int* **2018**:1467143.
- Martignoni M, Groothuis GM, and de Kanter R (2006) Species differences between mouse, rat, dog, monkey and human CYP-mediated drug metabolism, inhibition and induction. *Expert Opin Drug Metab Toxicol* **2**:875–894.
- Modica-Napolitano JS, Bharath LP, Hanlon AJ, and Hurley LD (2019) The anticancer agent elesclomol has direct effects on mitochondrial bioenergetic function in isolated mammalian mitochondria. *Biomolecules* **9**:298.
- Qin J, Li R, Raes J, Arunugam M, Burgdorf KS, Manichanh C, Nielsen T, Pons N, Levenez F, Yamada T et al.; MetaHIT Consortium (2010) A human gut microbial gene catalogue established by metagenomic sequencing. *Nature* **464**:59–65.
- Roberts AB, Wallace BD, Venkatesh MK, Mani S, and Redinbo MR (2013) Molecular insights into microbial β -glucuronidase inhibition to abrogate CPT-11 toxicity. *Mol Pharmacol* **84**:208–217.
- Savage N (2020) The complex relationship between drugs and the microbiome. *Nature* **577**:S10–S11.
- Selwyn FP, Cui JY, and Klaassen CD (2015) RNA-Seq quantification of hepatic drug processing genes in germ-free mice. *Drug Metab Dispos* **43**:1572–1580.
- Sender R, Fuchs S, and Milo R (2016) Revised estimates for the number of human and bacteria cells in the body. *PLoS Biol* **14**:e1002533.
- Sepich-Poore GD, Zitvogel L, Straussman R, Hasty J, Wargo JA, and Knight R (2021) The microbiome and human cancer. *Science* **371**:eaab4552.
- Sharma A, Buschmann MM, and Gilbert JA (2019) Pharmacomicrobiomics: the holy grail to variability in drug response? *Clin Pharmacol Ther* **106**:317–328.
- Sommer F, Nookaew I, Sommer N, Fogelstrand P, and Bäckhed F (2015) Site-specific programming of the host epithelial transcriptome by the gut microbiota. *Genome Biol* **16**:62.
- Staudinger JL, Goodwin B, Jones SA, Hawkins-Brown D, MacKenzie KI, LaTour A, Liu Y, Klaassen CD, Brown KK, Reinhard J et al. (2001) The nuclear receptor PXR is a lithocholic acid sensor that protects against liver toxicity. *Proc Natl Acad Sci USA* **98**:3369–3374.
- Toda T, Ohi K, Kudo T, Yoshida T, Ikarashi N, Ito K, and Sugiyama K (2009a) Ciprofloxacin suppresses Cyp3a in mouse liver by reducing lithocholic acid-producing intestinal flora. *Drug Metab Pharmacokinet* **24**:201–208.
- Toda T, Saito N, Ikarashi N, Ito K, Yamamoto M, Ishige A, Watanabe K, and Sugiyama K (2009b) Intestinal flora induces the expression of Cyp3a in the mouse liver. *Xenobiotica* **39**:323–334.
- Togao M, Kawakami K, Otsuka J, Wagai G, Ohta-Takada Y, and Kado S (2020) Effects of gut microbiota on in vivo metabolism and tissue accumulation of cytochrome P450 3A metabolized drug: midazolam. *Biopharm Drug Dispos* **41**:275–282.
- Valdes AM, Walter J, Segal E, and Spector TD (2018) Role of the gut microbiota in nutrition and health. *BMJ* **361**:k2179.
- Van Boeckel TP, Gandra S, Ashok A, Caudron Q, Grenfell BT, Levin SA, and Laxminarayan R (2014) Global antibiotic consumption 2000 to 2010: an analysis of national pharmaceutical sales data. *Lancet Infect Dis* **14**:742–750.
- Wu B, Chen M, Gao Y, Hu J, Liu M, Zhang W, and Huang W (2019) In vivo pharmacodynamic and pharmacokinetic effects of metformin mediated by the gut microbiota in rats. *Life Sci* **226**:185–192.
- Yip LY and Chan EC (2015) Investigation of host-gut microbiota modulation of therapeutic outcome. *Drug Metab Dispos* **43**:1619–1631.
- Zhang YT, Zhang DF, Ge NY, Zhu GH, Hao C, Zhang Y, and Chen RJ (2016) Effect of evoidamine on CYP enzymes in rats by a cocktail method. *Pharmacology* **97**:218–223.
- Zhou Y, Tu Y, Zhou Q, Hua A, Geng P, Chen F, Han A, Liu J, Dai D, Wang S et al. (2020) Evaluation of acetaminophen inhibition potential against cytochrome P450 in vitro and in vivo. *Chem Biol Interact* **329**:109147.
- Zuber R, Anzenbacherová E, and Anzenbacher P (2002) Cytochromes P450 and experimental models of drug metabolism. *J Cell Mol Med* **6**:189–198.

Address correspondence to: Qing Li, Department of Clinical Pharmacology, Xiangya Hospital, Central South University, 110 Xiangya Road, Changsha, Hunan 410078, China. E-mail: liqing9251026@csu.edu.cn; or Xiong Li, Key Specialty of Clinical Pharmacy, The First Affiliated Hospital, Guangdong Pharmaceutical University, 19 Nonglinxia Road, Yuexiu District, Guangzhou, Guangdong, China. E-mail: lixiong@gdpu.edu.cn.